



Published in final edited form as:

Hum Mutat. 2020 July ; 41(7): 1321–1328. doi:10.1002/humu.24019.

Disease-causing Missense Mutations within the N-terminal Transmembrane Domain of GlcNAc-1-phosphotransferase Impair Endoplasmic Reticulum Translocation or Golgi Retention

Wang-Sik Lee, Benjamin C. Jennings, Balraj Doray, Stuart Kornfeld[#]

Department of Internal Medicine, Washington University School of Medicine, St. Louis, Missouri 63110, USA

Abstract

Transport of newly synthesized lysosomal enzymes to the lysosome requires tagging of these enzymes with the mannose 6-phosphate moiety by UDP-GlcNAc:lysosomal enzyme N-acetylglucosamine-1-phosphotransferase (GlcNAc-1-phosphotransferase), encoded by two genes, *GNPTAB* and *GNPTG*. *GNPTAB* encodes the α and β subunits, which are initially synthesized as a single precursor that is cleaved by Site-1 protease in the Golgi. Mutations in this gene cause the lysosomal storage disorders mucopolipidosis II (MLII) and mucopolipidosis III $\alpha\beta$ (MLIII $\alpha\beta$). Two recent studies have reported the first patient mutations within the N-terminal transmembrane domain (TMD) of the α subunit of GlcNAc-1-phosphotransferase that cause either MLII or MLIII $\alpha\beta$. Here, we demonstrate that two of the MLII missense mutations, c.80T>A (p.Val27Asp) and c.83T>A (p.Val28Asp), prevent the cotranslational insertion of the nascent GlcNAc-1-phosphotransferase polypeptide chain into the endoplasmic reticulum. The remaining four mutations, one of which is associated with MLII, c.100G>C (p.Ala34Pro), and the other three with MLIII $\alpha\beta$, c.70T>G (p.Phe24Val), c.77G>A (p.Gly26Asp), and c.107A>C (p.Glu36Pro), impair retention of the catalytically active enzyme in the Golgi with concomitant mistargeting to endosomes/lysosomes. Our results uncover the basis for the disease phenotypes of these patient mutations and establish the N-terminal TMD of GlcNAc-1-phosphotransferase as an important determinant of Golgi localization.

Keywords

GlcNAc-1-phosphotransferase; mucopolipidosis II; mucopolipidosis III $\alpha\beta$; transmembrane domain; ER translocation; Golgi retention

INTRODUCTION

The degradation of intracellular and endocytosed materials within the lysosome is dependent on the proper targeting of 60 or so acid hydrolases to this organelle. Defects in this transport

[#]To whom correspondence should be addressed: Department of Internal Medicine, Hematology Division, Campus Box 8125, Washington University School of Medicine, 660 South Euclid Avenue, St. Louis, MO 63110, USA, Tel.: (314) 362 8803; Fax: (314) 362 8826; skornfel@wustl.edu.

CONFLICTS OF INTEREST

The authors declare no conflicts of interest in this study.

pathway give rise to a number of diseases collectively known as Lysosomal Storage Disorders (Parenti, Andria, & Ballabio, 2015). Most notable among these are mucopolipidosis II (MLII) (MIM# 252500) and mucopolipidosis III $\alpha\beta$ (MLIII $\alpha\beta$) (MIM# 252600), which result from mutations in the *GNPTAB* gene (RefSeq NM_024312.5) that encodes the α and β subunits of the enzyme UDP-GlcNAc:lysosomal enzyme GlcNAc-1-phosphotransferase (GlcNAc-1-phosphotransferase; EC 2.7.8.17) (Kudo, Brem, & Canfield, 2006). The α and β subunits of GlcNAc-1-phosphotransferase are initially synthesized as an inactive α/β precursor polypeptide chain in the endoplasmic reticulum (ER). The precursor is then transported to the *cis*-Golgi where it undergoes cleavage by Site-1 protease (S1P) into the individual α and β subunits, a step that is essential for catalytic activation (Marschner, Kollmann, Schweizer, Braulke, & Pohl, 2011).

GlcNAc-1-phosphotransferase performs the initial and most crucial step in the generation of the mannose 6-phosphate (Man-6-P) recognition marker on newly synthesized lysosomal acid hydrolases. This marker allows for high-affinity binding to Man-6-P receptors (MPRs) in the *trans*-Golgi network and transport to the endo-lysosomal system (Kornfeld, 1986). The steady-state localization of GlcNAc-1-phosphotransferase in the *cis*-Golgi is imperative for the fidelity of this process, as illustrated by mutations in the N-terminal cytoplasmic tail (N-tail) of the enzyme which lead to mislocalization to lysosomes, resulting in MLIII $\alpha\beta$ (van Meel, Qian, & Kornfeld, 2014).

To date, there are no studies on the role of the N-terminal transmembrane domain (TMD) of GlcNAc-1-phosphotransferase in Golgi localization. Two recent publications have reported the first patient mutations within the N-terminal TMD of GlcNAc-1-phosphotransferase which lead to MLII or MLIII $\alpha\beta$, although the cellular consequences of these mutations was not addressed (Velho et al., 2019; Wang et al., 2019). Here, we report on the functional characterization of these missense mutations, showing that four of the six mutations affect Golgi retention of GlcNAc-1-phosphotransferase while the other two prevent insertion into the ER.

MATERIALS AND METHODS

Reagents and Antibodies

UDP-[^3H]GlcNAc (20-45 Ci/mmol) was purchased from Perkin Elmer (Boston, MA). Mouse anti-V5 monoclonal antibody (Cat #46-0705) was obtained from Thermo Fisher (Waltham, MA) while anti-giantin rabbit polyclonal antibody (Cat # 924302) was from BioLegend (San Diego, CA). Endo Hf was purchased from New England BioLabs (Ipswich, MA). Methyl α -D-mannopyranoside (α -MM) was from Sigma-Aldrich (St. Louis, MO).

DNA Constructs

The full-length human GlcNAc-1-phosphotransferase-V5/His constructs in pcDNA6 has been described (Qian et al., 2015). Constructs with mutations in the N-terminal TMD were generated by 2-step overlap-extension PCR wherein the WT DNA fragment encoding the first 364 aa of GlcNAc-1-phosphotransferase was swapped for the same size fragment

harboring the individual mutation. DNA sequencing was performed to ensure that only the desired site was mutated within the swapped DNA fragment.

Cell Lines

HEK 293 and HeLa cells (ATCC) were maintained in DMEM containing 0.11 g/L sodium pyruvate and 4.5 g/L glucose, supplemented with 10% (vol/vol) FBS, 100,000 U/L penicillin, 100 mg/L streptomycin and 2 mM L-glutamine. *GNPTAB*^{-/-} HeLa cells were maintained under similar conditions except that 20% instead of 10% FBS was used.

GlcNAc-1-phosphotransferase Assay

Constructs encoding the WT and TMD mutant precursors were expressed in HEK 293 cells by transfection with the jetOPTIMUS transfection reagent from Polyplus (Illkirch, France) according to the manufacturer's protocol. Cells in 6-well plates were harvested 48 h post-transfection and lysed in 100 μ l of buffer A (25 mM Tris-Cl, pH 7.2, 150 mM NaCl, 1% Triton-X 100 and protease inhibitor cocktail). 30 μ g of each cell lysate was incubated for 2 h at 37 °C in a buffer containing 100mM α -methyl mannoside, 50 mM Tris-HCl, pH 7.4, 10 mM MgCl₂, 10 mM MnCl₂, 75 μ M UDP-[³H]GlcNAc (1 μ Ci), and 2 mg/mL bovine serum albumin in a final volume of 50 μ l. The reactions were terminated by addition of 950 μ l of 5 mM EDTA, pH 8.0. The sample was applied to a 1 mL column of QAE-Sephadex (GE Healthcare, Chicago, IL) equilibrated with 2 mM Tris base, pH 8.0. The column was washed with 5 mL of 2 mM Tris base and the phosphorylated products were eluted with 5 mL of 2 mM Tris base containing 30 mM NaCl. The incorporated [³H]GlcNAc-P was determined by addition of 8.5 mL of EcoLite scintillation fluid (MP Biomedicals Inc., Irvine, CA). The background activity in non-transfected cells less than 1% of that obtained with cells transfected with WT GlcNAc-1-phosphotransferase cDNA.

CI-MPR Affinity Chromatography and Lysosomal Enzyme Assays

The preparation of the cation-independent MPR (CI-MPR) beads from soluble bovine CI-MPR purified from FBS has been described (Valenzano, Remmler, & Lobel, 1995). Equivalent amounts of cell extract from 2-day transfected *GNPTAB*^{-/-} HeLa cells were incubated with CI-MPR affinity beads, washed twice with buffer and then assayed for bound lysosomal enzymes as previously described (Gelfman et al., 2007). Briefly, β -hexosaminidase (β -Hex) and β -galactosidase (β -Gal) were assayed with 5 mM 4-methylumbelliferyl(MU)-N-acetyl- β -d-glucosaminide (Sigma-Aldrich) and 5 mM 4-MU- β -d-galactopyranoside (Calbiochem, San Diego, CA), respectively, in 50 mM citrate buffer containing 0.5% Triton X-100 (pH 4.5). The activity of β -glucuronidase (GUSB) was assayed with 5 mM 4-MU- β -d-glucuronide (Calbiochem) in 0.1 M Na-acetate buffer containing 0.5% Triton X-100 (pH 4.6). The activity of β -mannosidase (β -Man) was assayed with 5 mM 4-MU- β -d-mannopyranoside (Sigma-Aldrich) in 50 mM Na-citrate buffer containing 0.5% Triton X-100 (pH 5.0).

Immunofluorescence Microscopy

To visualize the subcellular localization of the WT and mutant GlcNAc-1-phosphotransferase, the various constructs were transfected into HeLa cells using the

jetOPTIMUS transfection reagent. The cells were fixed 24-36 h post-transfection with 4% formaldehyde (Sigma-Aldrich) for 10 min, permeabilized and blocked with PBS containing 0.4% (v/v) Triton X-100 and 2% IgG free BSA (Jackson ImmunoResearch) for 1 h, and then probed with the indicated combinations of antibodies in PBS containing 0.1% Triton X-100 and 0.5% BSA. For observation of non-permeabilized cells, TritonX-100 was omitted at every step. The processed cells were mounted in ProLong® Gold antifade mounting medium (Life Technologies), and the images were acquired with an LSM880 confocal microscope (Carl Zeiss Inc., Peabody, MA). Images were analyzed by Image J software (Fiji).

Immunoblotting

Proteins resolved by SDS-PAGE under reducing conditions were transferred to nitrocellulose membrane and detected with antibodies as described in the figure legends. The indicated amounts of whole cell extract were loaded on the gels.

RESULTS

Transmembrane mutations identified in patients with MLII/ MLIII $\alpha\beta$ impair the activity of GlcNAc-1-phosphotransferase.

In order to assess the effect of the disease-causing missense mutations on the activity of GlcNAc-1-phosphotransferase, cDNAs encoding either wild-type (WT) enzyme or the various mutants (Figure 1a) were transfected into HEK 293 cells. All constructs were appended with a C-terminal V5 epitope sequence. Catalytic activity was measured 48 h post-transfection using an equivalent amount of whole cell lysates in an *in vitro* assay in which the simple sugar α -MM served as the substrate. Four of the six variants, c.70T>G (p.Phe24Val), c.77G>A (p.Gly26Asp), c.100G>C (p.Ala34Pro), and c.107A>C (p.Glu36Pro), resulted in mutant proteins displaying catalytic activity ranging from 25-65% of the WT value (which is set at 100%), whereas the c.80T>A (p.Val27Asp) and c.83T>A (p.Val28Asp) mutations resulted in mutant proteins showing virtually no activity (Figure 1b).

We next analyzed expression of the WT and mutant proteins by immunoblotting. Cell lysates (10 μ g) from HEK cells transfected with the various constructs were resolved on an SDS gel, with the exception of the p.Val27Asp and p.Val28Asp mutants, in which case 40 μ g of cell lysate was loaded due to poor expression of the two mutants. The proteins were then transferred to nitrocellulose and probed with the anti-V5 antibody. The V5-epitope is at the C-terminus of the β subunit (Figure 1a), so both inactive α/β precursor and the active β subunit will be detected by immunoblotting but not the α subunit. As shown in Figure 1c, the amount of the processed β subunit of the p.Phe24Val mutant was decreased marginally relative to WT GlcNAc-1-phosphotransferase, while the decrease was much more substantial with the p.Gly26Asp, p.Ala34Pro and p.Glu36Pro mutants, in good agreement with the enzyme activity data wherein p.Phe24Val displayed the highest activity among the patient mutants (Figure 1b). The level of the inactive α/β precursor was not substantially different between WT and the p.Phe24Val, p.Gly26Asp, p.Ala34Pro and p.Glu36Pro mutants (Figure 1c). On the other hand, the lysates of the p.Val27Asp and p.Val28Asp transfected cells had dramatically decreased levels of the inactive α/β precursor and no

detectable β subunit, which explains the complete lack of enzyme activity of these mutants. We also observed that the α/β precursor of these mutants migrated faster on the SDS gel (Figure 1c, *), consistent with a lack of N-linked glycosylation. This suggested a block in the translocation of the nascent p.Val27Asp and p.Val28Asp mutant polypeptide chains into the lumen of the ER where the α/β precursor acquires N-linked high mannose glycan chains. To test this hypothesis, endoglycosidase H (Endo H) treatment, which removes N-linked high mannose or hybrid type glycans from glycoproteins, was performed with WT GlcNAc-1-phosphotransferase alongside the p.Val28Asp and the p.Ala34Pro mutants (Figure 1d). Whereas the WT and p.Ala34Pro precursor chains shifted down with Endo H treatment as a result of removal of the associated N-glycan chains, no shift was seen with the p.Val28Asp mutant, consistent with an inability of this mutant to be inserted into the lumen of the ER. Failure to deliver the newly synthesized p.Val27Asp and p.Val28Asp mutants to the ER could also explain the low expression observed in the western blot of these two mutants, as the non-glycosylated nascent polypeptides would not be expected to fold properly in the cytosol, leading to their degradation.

The p.Phe24Val, p.Gly26Asp, p.Ala34Pro and p.Glu36Pro mutants are poorly retained in the Golgi.

Since GlcNAc-1-phosphotransferase is initially synthesized as an inactive α/β precursor in the ER and requires transport to the cis-Golgi for cleavage into the α and β subunits by S1P for activation, we considered two possibilities to account for the decrease in activity of the p.Phe24Val, p.Gly26Asp, p.Ala34Pro and p.Glu36Pro mutants; i) the mutants exit the ER poorly and consequently are not activated by S1P cleavage, or ii) the mutants are transported to the *cis*-Golgi and activated but their retention in this compartment is impaired, resulting in inactivation of the mutant enzymes in the endo-lysosomal compartment and/or transport to the cell-surface.

In order to distinguish between these two possibilities, HeLa cells were transfected with either WT or mutant GlcNAc-1-phosphotransferase cDNAs, and the cells were processed for confocal immunofluorescence microscopy 24-36 h post transfection. As described previously, the localization of WT GlcNAc-1-phosphotransferase in HeLa cells was impacted by the level of expression of the protein (van Meel et al., 2014). High expression resulted in GlcNAc-1-phosphotransferase being detected in the ER in addition to the Golgi (not shown). Moderate to low expression, however, resulted in the WT enzyme being detected primarily in the Golgi where it colocalized with the *cis*-Golgi marker giantin (Figure 2). The p.Phe24Val, p.Gly26Asp, p.Ala34Pro, and p.Glu36Pro mutants, on the other hand, displayed a predominantly punctate appearance (Figure 2) with low levels in the Golgi, similar to observations with N-tail mutants (Liu, Doray, & Kornfeld, 2018; van Meel et al., 2014). None of these TMD mutants showed the characteristic ER pattern of staining, as was the case with the p.R334Q mutant which served as a control for ER retention (Figure 2) (Qian et al., 2015). It is of note that expression of the p.Val27Asp and p.Val28Asp mutants was hardly detectable by immunofluorescence microscopy, and in the few cells where any signal was observed, only a faint diffuse cytoplasmic staining was observed (not shown). Taken together, these data demonstrate that patient mutations within the N-terminal TMD of GlcNAc-1-phosphotransferase either prevent translocation of the mutants into the

ER (p.Val27Asp and p.Val28Asp), or impair retention of the mutant proteins in the Golgi (p.Phe24Val, p.Gly26Asp, p.Ala34Pro and p.Glu36Pro).

The p.Phe24Val, p.Gly26Asp, p.Ala34Pro and p.Glu36Pro mutants are degraded in the lysosome.

We previously established that punctae seen in immunofluorescence microscopy of the N-tail mutants of GlcNAc-1-phosphotransferase are, for the most part, components of the endo-lysosomal compartment (Liu et al., 2018; van Meel et al., 2014). We also showed that treatment of transfected cells with Bafilomycin A1 significantly increased the amount of the active β subunit of the mutants that are impaired in Golgi retention by blocking exit from this organelle. To determine if this is the case with the TMD mutants, Bafilomycin a1 was added to transfected HEK 293 cells 24 hr post-transfection at a final concentration of 100 nM for 6 hours. Cell lysates were then assayed for GlcNAc-1-phosphotransferase catalytic activity and protein levels were determined by immunoblotting. Figure 3a shows that WT GlcNAc-1-phosphotransferase as well as the p.Phe24Val, p.Gly26Asp, p.Ala34Pro and p.Glu36Pro mutants all showed an increase in activity after bafilomycin treatment, with the increase ranging from 1.8-fold for WT to 2.4-5-fold for the mutants. The enzyme activity data were corroborated by immunoblot analysis which showed increased amounts of the active β subunit following bafilomycin treatment for WT, p.Phe24Val, p.Gly26Asp, p.Ala34Pro and p.Glu36Pro (Figure 3b). These results provide additional evidence that mutations in the N-terminal TMD of GlcNAc-1-phosphotransferase that impair Golgi retention lead to transport to lysosomes for degradation. In contrast, the lysates of the p.Val27Asp and p.Val28Asp mutants had no activity even in the presence of bafilomycin (Figure 3a), since the delivery of these mutants to the ER lumen is affected.

Effect of TMD mutations on acid hydrolase phosphorylation.

We have reported that the acid hydrolases from *GNPTAB*^{-/-} HeLa cells have less than 1% binding to CI-MPR beads relative to the acid hydrolases from WT HeLa cells, reflecting the lack of GlcNAc-1-phosphotransferase activity (van Meel et al., 2016). We next transfected *GNPTAB*^{-/-} HeLa cells with either WT or mutant cDNAs in order to assess the ability of the various TMD mutants to restore phosphorylation to four different lysosomal enzymes when compared to WT GlcNAc-1-phosphotransferase. As shown in Table 1, the binding to the CI-MPR beads, a measure of the extent of phosphorylation, was modestly decreased with the p.Gly26Asp, p.Asp34Pro, and p.Glu36Pro mutants, whereas the p.Phe24Val mutant behaved like WT GlcNAc-1-phosphotransferase in this assay. As expected, there was no significant activity with the p.Val27Asp and p.Val28Asp mutants. It must be noted that the transfected HeLa cells express between 50-100 fold the endogenous level of GlcNAc-1-phosphotransferase. Consequently, the level of the various mutants should be more than adequate to maintain the WT level of acid hydrolase phosphorylation. However, only in the case of p.Phe24Val is this observed. The likely explanation is that much of the mutant enzymes have escaped the Golgi, leaving behind an inadequate amount of enzyme to phosphorylate the acid hydrolases in the Golgi.

The N-terminal TMD of GlcNAc-1-phosphotransferase functions as an autonomous Golgi localization signal.

We have shown that the cytoplasmic N-tail of GlcNAc-1-phosphotransferase harbors sufficient information on its own to direct a chimera containing the TMD of a type II plasma membrane protein, sucrase isomaltase (SI), and luminal green fluorescent protein (GFP) to the Golgi (PT-SI-GFP) (Figures 4a & b) (Liu et al., 2018). In contrast, the chimeric protein containing both the N-tail and TMD of SI fused to GFP (SI-SI-GFP) (Figure 4a) lacked Golgi localization (Figure 4b)(Liu et al., 2018) and showed strong cell surface expression, as seen with the anti-GFP staining of transfected non-permeabilized HeLa cells (Figure 4c). We next asked if the N-terminal TMD of GlcNAc-1-phosphotransferase alone is sufficient to direct a chimeric protein containing the N-tail of SI and luminal GFP to the Golgi (SI-PT-GFP) (Figure 4a). As shown by the confocal immunofluorescence microscopy images, SI-PT-GFP displayed good colocalization with the *cis*-Golgi marker giantin, very similar to PT-SI-GFP (Figure 4b). This result shows that the N-terminal TMD alone of GlcNAc-1-phosphotransferase is sufficient for Golgi localization. The Asp34Pro mutant of SI-PT-GFP, on the other hand, failed to colocalize with giantin (Figure 4b). The lack of a cell surface signal with the anti-GFP antibody (Figure 4c) suggests that this mutant is either retained in the ER and/or present in the endosomes/lysosomes.

DISCUSSION

The results presented here are the first to analyze the consequences of missense mutations within the N-terminal TMD of GlcNAc-1-phosphotransferase that were recently identified in patients with MLII/ MLIII $\alpha\beta$ (Velho et al., 2019; Wang et al., 2019). Our data establish that two of the mutations, namely p.Val27Asp and p.Val28Asp, that cause the more severe form of the disease (MLII), prevent the insertion of the nascent polypeptide chain into the ER lumen, and have no detectable enzyme activity. Since the α subunit of GlcNAc-1-phosphotransferase has a similar configuration to a type II transmembrane protein, its TMD serves as an uncleaved signal peptide/membrane anchor (SA). This domain interacts with signal recognition particle (SRP) to form a SRP-ribosome-nascent polypeptide complex that subsequently associates with the translocon on the surface of the rough ER, followed by translocation of the nascent protein into the lumen of that organelle (Egea, Stroud, & Walter, 2005). Our data indicate that valine 27 and valine 28 are critical residues of the SA domain of GlcNAc-1-phosphotransferase, and that mutation of either valine to aspartate likely abrogates SRP recognition by the TMD as it emerges from the ribosome. In this case, the translated α/β precursor polypeptide chain will not be co-translationally inserted into the ER lumen, which is borne out by our finding that the p.Val27Asp and p.Val28Asp mutants lack glycosylation and are present at very low levels in the cell. Presumably, these mutant GlcNAc-1-phosphotransferases are unable to fold in the cytosol and are degraded.

The remaining four mutations, including one that causes MLII (p.Ala34Pro), together with the three that cause MLIII $\alpha\beta$ (p.Phe24Val, p.Gly26Asp, and p.Glu36Pro), impair retention in the Golgi. It has been reported that TMDs vary, depending on their organelle of residence, both in length and composition (Sharpe, Stevens, & Munro, 2010; Welch & Munro, 2019). These differences presumably impact how well the TMDs fit into the lipid bilayer of an

organelle. It seems likely that the missense mutations described here impair the ability of the mutant TMD to interact properly with the lipids of the Golgi bilayer, resulting in an unstable situation that allows the mutant protein to escape the Golgi. An alternate explanation is that the N-terminal TMD of GlcNAc-1-phosphotransferase interacts with another Golgi protein to maintain its proper localization and the various mutations impair this interaction, resulting in the escape of the mutant protein from the Golgi (Schoberer et al., 2019; Sharpe et al., 2010; Welch & Munro, 2019). Further work will be required to clarify this situation.

The failure of these mutant enzymes to either be delivered to the ER for onward trafficking to the Golgi, or efficiently retained in the Golgi, severely impacts their ability to generate the Man-6-P recognition marker on newly synthesized acid hydrolases. This, in turn, impairs the proper targeting of the latter to lysosomes, which results in the development of a lysosomal storage disorder. While our study clearly reveals two distinct mechanisms that contribute to the pathogenicity of these mutations, a correlation of our functional data with the clinical outcome of the individual patients is not precise. For instance, both the p.Ala34Pro and p.Glu36Pro mutants are poorly retained in the Golgi and display around 20% GlcNAc-1-phosphotransferase activity compared to WT, yet the patient with the p.Ala34Pro mutation was diagnosed with MLII (Wang et al., 2019), while the patient with the p.Glu36Pro mutation was diagnosed with MLIII $\alpha\beta$ (Velho et al., 2019). In the case of the former, it was reported that the second *GNPTAB* allele of the patient also had a mutation (c.136C>T; p.Arg46X) which resulted in the codon for arginine changing into a termination codon. No data is available to show if the latter patient also had a biallelic mutation of the *GNPTAB* gene, which makes it difficult to establish accurate genotype-phenotype correlations. Also, the clinical distinction between MLII and MLIII $\alpha\beta$ is not always precise, and in fact, an intermediate MLII/MLIII $\alpha\beta$ phenotype has been described for a cohort of eight patients who share the c.10A>C (p.Lys4Glu) mutation in the *GNPTAB* gene (Leroy et al., 2014). In addition, the *in vitro* GlcNAc-1-phosphotransferase activities reported in this study were assayed with whole cell extracts from cells transfected with either WT or mutant cDNAs. The N-terminal TMD mutants that exit the Golgi and are observed in punctae have yet to be degraded in the lysosome and are likely to be catalytically active and contribute to the total enzyme activity measured in cell lysates. This would lead to an over-estimation of the functional catalytic activity of these mutants since *in vivo*, only Golgi-localized GlcNAc-1-phosphotransferase is able to act on its endogenous substrates. A case in point is the p.Phe24Val mutant, which had a little over 60% of WT catalytic activity in our assay. Even if the second allele of this patient harbored a totally inactivating mutation, it would be hard to reconcile the disease condition of the patient with 30% normal activity, unless a significant fraction of the activity we observed is due to this mutant enzyme being present in a post-Golgi compartment, in agreement with our immunofluorescence microscopy data. An interrogation of the *GNPTAB* gene using the gnomAD browser (<https://gnomad.broadinstitute.org/>) revealed the c.70T>G (p.Phe24Val) variant to occur in 86 out of 279702 alleles that have been examined to date. While the low frequency of this variant would exclude the change as a polymorphism (Richards et al., 2015), we cannot rule out the possibility that c.70T>G (p.Phe24Val) is a benign variant as opposed to a pathogenic variant. The next significant hurdle is determining the mechanism by which the N-terminal TMD of GlcNAc-1-phosphotransferase functions as a Golgi retention signal.

ACKNOWLEDGMENTS

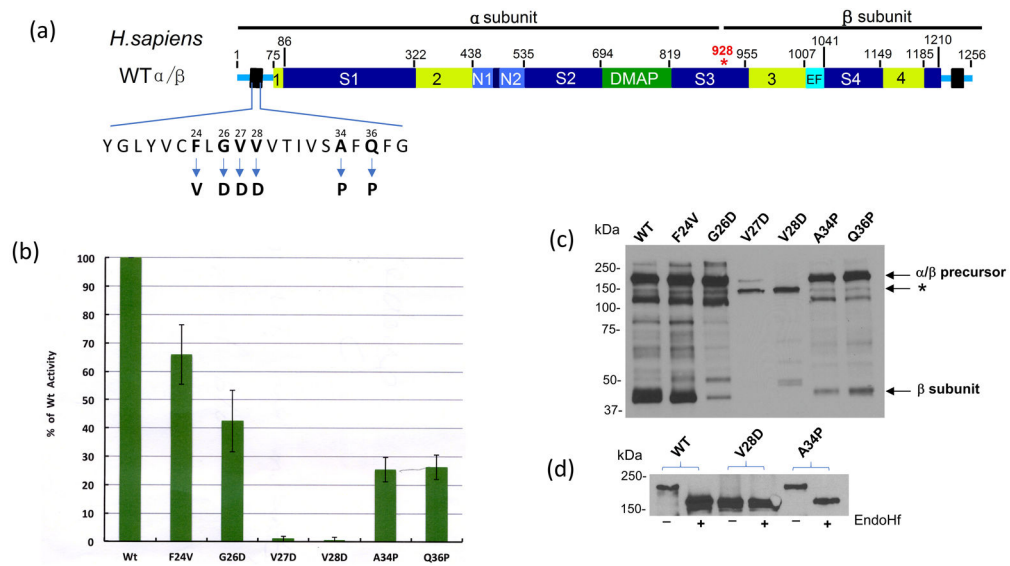
This work was supported by National Institutes of Health Grant 2R01CA008759-53 and the Yash Gandhi Foundation.

Funding information: National Institutes of Health Grant 2R01CA008759-53 and the Yash Gandhi Foundation.

REFERENCES

- Egea PF, Stroud RM, & Walter P (2005). Targeting proteins to membranes: structure of the signal recognition particle. *Curr Opin Struct Biol*, 15(2), 213–220. doi:10.1016/j.sbi.2005.03.007 [PubMed: 15837181]
- Gelfman CM, Vogel P, Issa TM, Turner CA, Lee WS, Kornfeld S, & Rice DS (2007). Mice lacking alpha/beta subunits of GlcNAc-1-phosphotransferase exhibit growth retardation, retinal degeneration, and secretory cell lesions. *Invest Ophthalmol Vis Sci*, 48(11), 5221–5228. doi:10.1167/iovs.07-0452 [PubMed: 17962477]
- Kornfeld S (1986). Trafficking of lysosomal enzymes in normal and disease states. *J Clin Invest*, 77(1), 1–6. doi:10.1172/JCI112262 [PubMed: 3003148]
- Kudo M, Brem MS, & Canfield WM (2006). Mucopolipidosis II (I-cell disease) and mucopolipidosis IIIA (classical pseudo-hurler polydystrophy) are caused by mutations in the GlcNAc-phosphotransferase alpha / beta -subunits precursor gene. *Am J Hum Genet*, 78(3), 451–463. doi:10.1086/500849 [PubMed: 16465621]
- Leroy JG, Sillence D, Wood T, Barnes J, Lebel RR, Friez MJ, ... Cathey SS (2014). A novel intermediate mucopolipidosis II/IIIalpha caused by GNPTAB mutation in the cytosolic N-terminal domain. *Eur J Hum Genet*, 22(5), 594–601. doi:10.1038/ejhg.2013.207 [PubMed: 24045841]
- Liu L, Doray B, & Kornfeld S (2018). Recycling of Golgi glycosyltransferases requires direct binding to coatomer. *Proc Natl Acad Sci U S A*, 115(36), 8984–8989. doi:10.1073/pnas.1810291115 [PubMed: 30126980]
- Marschner K, Kollmann K, Schweizer M, Bräulke T, & Pohl S (2011). A key enzyme in the biogenesis of lysosomes is a protease that regulates cholesterol metabolism. *Science*, 333(6038), 87–90. doi:10.1126/science.1205677 [PubMed: 21719679]
- Parenti G, Andria G, & Ballabio A (2015). Lysosomal storage diseases: from pathophysiology to therapy. *Annu Rev Med*, 66, 471–486. doi:10.1146/annurev-med-122313-085916 [PubMed: 25587658]
- Qian Y, van Meel E, Flanagan-Steet H, Yox A, Steet R, & Kornfeld S (2015). Analysis of mucopolipidosis II/III GNPTAB missense mutations identifies domains of UDP-GlcNAc:lysosomal enzyme GlcNAc-1-phosphotransferase involved in catalytic function and lysosomal enzyme recognition. *J Biol Chem*, 290(5), 3045–3056. doi:10.1074/jbc.M114.612507 [PubMed: 25505245]
- Richards S, Aziz N, Bale S, Bick D, Das S, Gastier-Foster J, ... Committee ALQA (2015). Standards and guidelines for the interpretation of sequence variants: a joint consensus recommendation of the American College of Medical Genetics and Genomics and the Association for Molecular Pathology. *Genet Med*, 17(5), 405–424. doi:10.1038/gim.2015.30 [PubMed: 25741868]
- Schoberer J, Liebminger E, Vavra U, Veit C, Grunwald-Gruber C, Altmann F, ... Strasser R (2019). The Golgi Localization of GnTI Requires a Polar Amino Acid Residue within Its Transmembrane Domain. *Plant Physiol*, 180(2), 859–873. doi:10.1104/pp.19.00310 [PubMed: 30971450]
- Sharpe HJ, Stevens TJ, & Munro S (2010). A comprehensive comparison of transmembrane domains reveals organelle-specific properties. *Cell*, 142(1), 158–169. doi:10.1016/j.cell.2010.05.037 [PubMed: 20603021]
- Valenzano KJ, Remmler J, & Lobel P (1995). Soluble insulin-like growth factor II/mannose 6-phosphate receptor carries multiple high molecular weight forms of insulin-like growth factor II in fetal bovine serum. *J Biol Chem*, 270(27), 16441–16448. doi:10.1074/jbc.270.27.16441 [PubMed: 7608216]
- van Meel E, Lee WS, Liu L, Qian Y, Doray B, & Kornfeld S (2016). Multiple Domains of GlcNAc-1-phosphotransferase Mediate Recognition of Lysosomal Enzymes. *J Biol Chem*, 291(15), 8295–8307. doi:10.1074/jbc.M116.714568 [PubMed: 26833567]

- van Meel E, Qian Y, & Kornfeld SA (2014). Mislocalization of phosphotransferase as a cause of mucopolipidosis III alpha/beta. *Proc Natl Acad Sci U S A*, 111(9), 3532–3537. doi:10.1073/pnas.1401417111 [PubMed: 24550498]
- Velho RV, Harms FL, Danyukova T, Ludwig NF, Friez MJ, Cathey SS, ... Pohl S (2019). The lysosomal storage disorders mucopolipidosis type II, type III alpha/beta, and type III gamma: Update on GNPTAB and GNPTG mutations. *Hum Mutat*, 40(7), 842–864. doi:10.1002/humu.23748 [PubMed: 30882951]
- Wang Y, Ye J, Qiu WJ, Han LS, Gao XL, Liang LL, ... Zhang HW (2019). Identification of predominant GNPTAB gene mutations in Eastern Chinese patients with mucopolipidosis II/III and a prenatal diagnosis of mucopolipidosis II. *Acta Pharmacol Sin*, 40(2), 279–287. doi:10.1038/s41401-018-0023-9 [PubMed: 29872134]
- Welch LG, & Munro S (2019). A tale of short tails, through thick and thin: investigating the sorting mechanisms of Golgi enzymes. *FEBS Lett*, 593(17), 2452–2465. doi:10.1002/1873-3468.13553 [PubMed: 31344261]

**Figure 1.**

(a) Schematic of human GlcNAc-1-phosphotransferase α/β subunit modular arrangement. The 4 regions shown in line together comprise the Stealth, an evolutionarily conserved domain which functions as the catalytic core of the protein. * indicates site of cleavage to generate the individual α and β subunits. Patient mutations within the N-terminal TMD are shown in bold. (b) GlcNAc-1-phosphotransferase activity toward the simple sugar α MM, using extracts of HEK 293 cells transfected with WT α/β precursor or the various point-mutation cDNAs. The vector-only transfected cell extract served as a control and activity was normalized to total protein concentration. (c) Western blot of WT α/β and mutants expressed in HEK 293 cells probed with the anti-V5 antibody. 10 μ g of each cell extract was loaded, with exception of the p.Val27Asp and p.Val28Asp mutants, in which case 40 μ g was loaded. (d) Western blot of WT and the indicated mutants analyzed after treatment with Endo Hf. Only the α/β precursor is shown here.

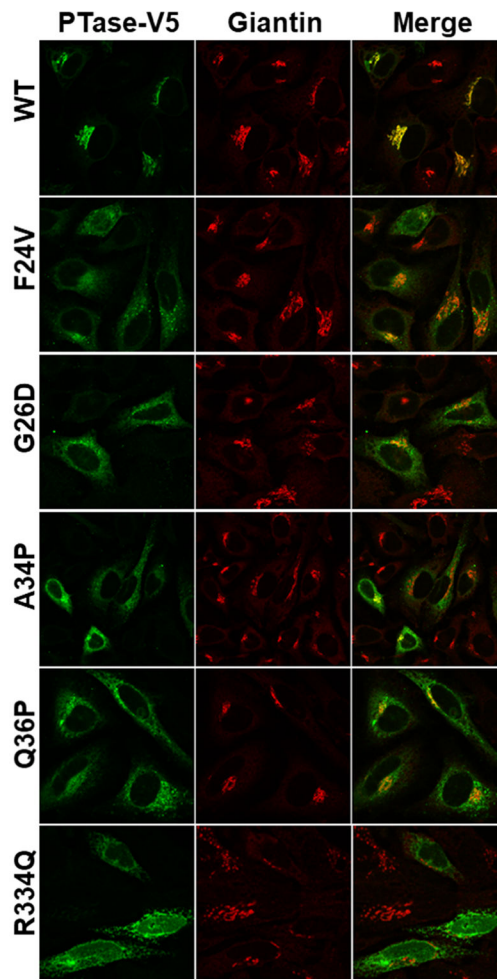


Figure 2. Subcellular localization of WT α/β precursor and mutants. Confocal immunofluorescence images of HeLa cells transfected with either WT α/β precursor, or the indicated mutant cDNAs, and colocalized with the Golgi marker giantin (see Materials and Methods).

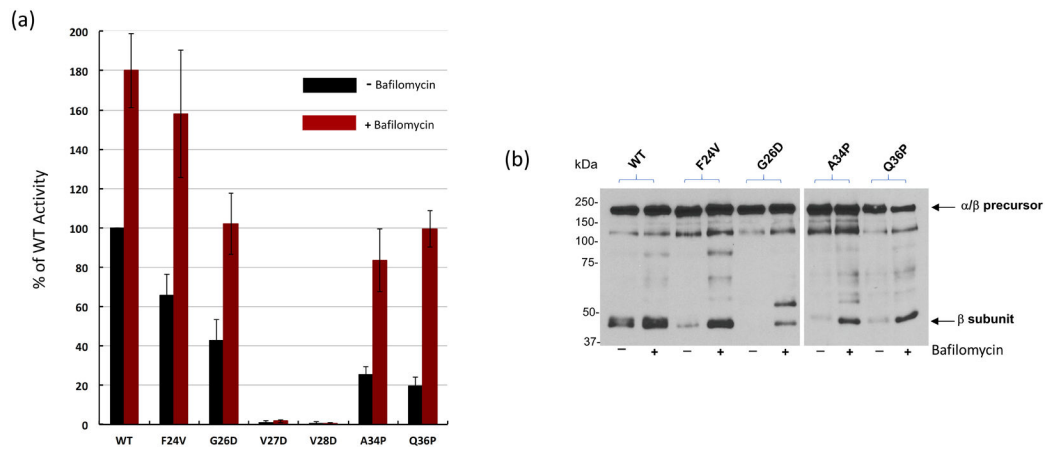


Figure 3.

Effect of bafilomycin treatment on activity of the TMD mutants. (a) HEK 293 cells transfected with WT α/β precursor or the various point-mutation cDNAs were treated 24 h post-transfection with either DMSO (control) or 100nM bafilomycin a1 for 6 h. Catalytic activity was then measured using equivalent amounts of whole cell extracts. The vector-only transfected cell extract served as a control. (b) Western blot (anti-V5) of HEK293 cells expressing WT or mutant GlcNAc-1-phosphotransferase treated with either DMSO (control) or 100 nM bafilomycin a1 for 6 h. The mature β subunits of all the mutants, except for p.Val27Asp and p.Val28Asp (not shown), increased after bafilomycin treatment.

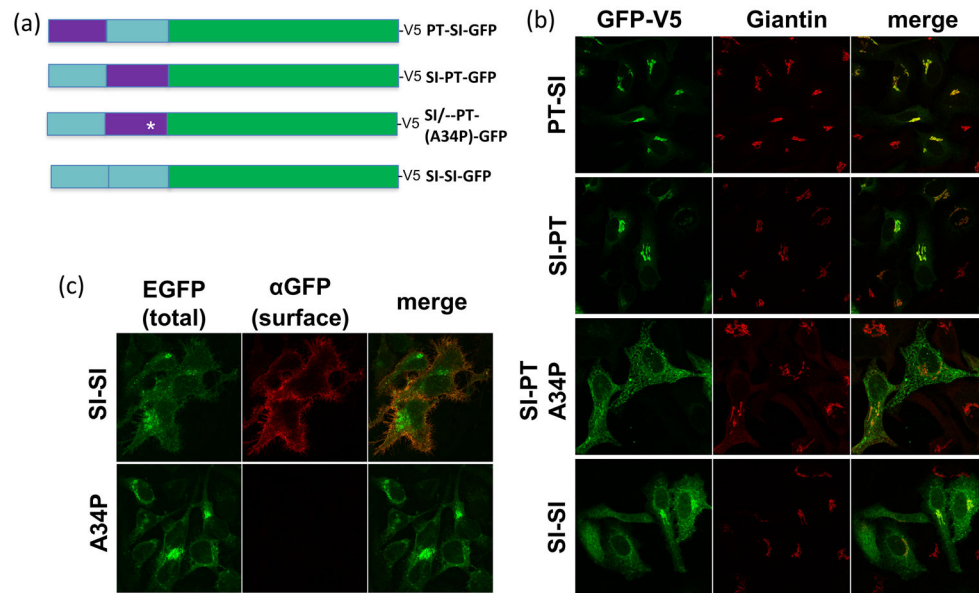


Figure 4. (a) Schematic of the various chimeric GFP (green)-V5 constructs encoding the N-tail or TMD of either GlcNAc-1-phosphotransferase (purple) or the plasma membrane protein, sucrase isomaltase (blue), as shown. (b) Immunofluorescence images of permeabilized HeLa cells transfected with the indicated chimeric GFP-V5 constructs, probed with the anti-V5 antibody (green) and colocalized with the Golgi marker giantin (red). (c) Immunofluorescence images of non-permeabilized HeLa cells transfected with either SI-SI-GFP-V5 or SI-PT (Asp34Pro)-GFP-V5 cDNA. Cells were probed with an anti-GFP antibody (red) and compared with native GFP fluorescence (green).

Table 1.

Lysosomal Enzyme Phosphorylation of TMD Mutants

Constructs	β - HEX	GUSB	β - Man	β - Gal
Wt	100%	100%	100%	100%
F24V	93	99	110	99
G26D	44	70	46	35
V27D	<2	<2	<2	<2
V28D	<2	<2	<2	<2
A34P	62	80	72	66
Q36P	60	75	75	54

Data are the mean of two independent transfections of the indicated cDNAs into HeLa *GNPTAB*^{-/-} cells. Following CI-MPR bead binding, the activities of the enzymes were assayed as described in Materials & Methods. WT activity is set at 100% after subtraction of background values from untransfected cells.